Cited2 is required for the proper formation of the hyaloid vasculature and for lens morphogenesis

Published in final edited form as:
Development. 2008 September ; 135(17): 2939–2948. doi:10.1242/dev.021097.

Cited2 is required for the proper formation of the hyaloid vasculature and for lens morphogenesis

Yu Chen[1], **Yong-qiu Doughman**[2], **Shi Gu**[1], **Andrew Jarrell**[1], **Shin-ichi Aota**[3], **Ales Cvekl**[4], **Michiko Watanabe**[2], **Sally L. Dunwoodie**[5], **Randall S. Johnson**[6], **Veronica van Heyningen**[7], **Dirk A. Kleinjan**[7], **David C. Beebe**[8], and **Yu-Chung Yang**[1,*]

1*Department of Biochemistry and Cancer Center, Case Western Reserve University School of Medicine, Cleveland, OH 44106, USA*

2*Department of Pediatrics, Rainbow Babies' and Children's Hospital, Case Western Reserve University School of Medicine, Cleveland, OH 44106, USA*

3*Developmental Biology, Graduate School of Frontier Biosciences, Osaka University, 1-3 Yamadaoka, Suita, Osaka 565-0871, Japan*

4*Departments of Ophthalmology and Visual Sciences and Molecular Genetics, Albert Einstein College of Medicine, Bronx, NY 10461, USA*

5*Developmental Biology Program, The Victor Chang Cardiac Research Institute, 384 Victoria Street, Darlinghurst, NSW 2010, Australia*

6*Molecular Biology Section, Division of Biological Sciences, School of Medicine, UCSD, La Jolla, CA 92093, USA*

7*MRC Human Genetics Unit, Western General Hospital, Edinburgh EH4 2XU, UK*

8*Department of Ophthalmology and Visual Sciences, Department of Cell Biology and Physiology, Washington University, St Louis, MO 63110, USA*

Abstract

Cited2 is a transcriptional modulator with pivotal roles in different biological processes. Cited2-deficient mouse embryos manifested two major defects in the developing eye. An abnormal corneal-lenticular stalk was characteristic of *Cited2*$^{-/-}$ developing eyes, a feature reminiscent of Peters' anomaly, which can be rescued by increased *Pax6* gene dosage in *Cited2*$^{-/-}$ embryonic eyes. In addition, the hyaloid vascular system showed hyaloid hypercellularity consisting of aberrant vasculature, which might be correlated with increased VEGF expression in the lens. Deletion of *Hif1a* (which encodes HIF-1α) in *Cited2*$^{-/-}$ lens specifically eliminated the excessive accumulation of cellular mass and aberrant vasculature in the developing vitreous without affecting the corneal-lenticular stalk phenotype. These in vivo data demonstrate for the first time dual functions for Cited2: one upstream of, or together with, Pax6 in lens morphogenesis; and another in the normal formation of the hyaloid vasculature through its negative modulation of HIF-1 signaling. Taken together, our study provides novel mechanistic revelation for lens morphogenesis and hyaloid vasculature formation and hence might offer new insights into the etiology of Peters' anomaly and ocular hypervascularity.

*Author for correspondence (e-mail: yu-chung.yang@case.edu).

Keywords

Cited2; Hyaloid vasculature; Lens development; Mouse

INTRODUCTION

Cited2 [Cbp/p300-interacting transactivator, with Glu/Asp-rich carboxy-terminal domain, 2] is one of the founding members of a family of transcriptional modulators (Shioda et al., 1997; Sun et al., 1998; Dunwoodie et al., 1998; Leung et al., 1999). Cited2 was previously named melanocyte-specific gene (MSG) related gene 1 (Mrg1; p35srj) (Shioda et al., 1997; Dunwoodie et al., 1998; Sun et al., 1998; Bhattacharya et al., 1999). It binds directly with high affinity to the first cysteine-histidine-rich (CH1) region of the transcription co-factors p300 and CBP. As a CBP/p300-dependent transcription factor, Cited2 functions as a negative regulator of hypoxia inducible factor 1 (HIF-1)-mediated signaling by competing with HIF-1α for binding to CBP/p300 (Bhattacharya et al., 1999). Cited2 physically interacts with several nuclear receptors and transcription factors, including PPAR (Ppara – Mouse Genome Informatics) (Tien et al., 2004), Hnf4α (Qu et al., 2007), Lhx2 (Glenn and Maurer, 1999), AP2 (Tcfap2) transcription factors (Bamforth et al., 2001) and Smad2/3 (Chou et al., 2006). Cited2 is also induced by many biological stimuli such as cytokines, serum and lipopolysaccharide in different cell types (Sun et al., 1998). Overexpression of Cited2 in Rat1 cells results in loss of cell contact inhibition, anchorage-independent growth and tumor formation in nude mice, demonstrating that *Cited2* is a transforming gene (Sun et al., 1998). These initial in vitro studies underscore the potential roles of Cited2 in different biological processes.

Deletion of *Cited2* results in embryonic lethality in mid- to late gestation, with embryos displaying cardiac malformations, neural tube defects, adrenal agenesis (Barbera et al., 2002; Bamforth et al., 2001; Yin et al., 2002; Val et al., 2007), left-right patterning defects (Weninger et al., 2005; Bamforth et al., 2004), placental defects (Withington et al., 2006), liver developmental defects (Qu et al., 2007) and defective fetal hematopoiesis (Chen et al., 2007). Further mechanistic studies have provided evidence that Cited2 plays pivotal roles in these processes through its transcriptional modulator functions for HIF-1 (Yin et al., 2002; Xu et al., 2007), AP2α (Tcfap2α – Mouse Genome Informatics) signaling (Bamforth et al., 2001; Bamforth et al., 2004), Hnf4α (Qu et al., 2007) and through other, as yet unknown, mechanisms.

The potential involvement of Cited2 in eye development was suggested by irregularly shaped pupils typical of Cited2-deficient embryos at 13.5 days post-coitum (dpc) (Yin et al., 2002). In this report, we show for the first time that Cited2 deficiency results in abnormal corneal-lenticular stalk formation and vitreous hypercellularity consisting of aberrant vasculature in the developing eye. We further demonstrate that Cited2 is an upstream positive regulator of Pax6 expression in the lens; this regulation is the mechanism that underlies the corneal-lenticular stalk formation resulting from Cited2 deficiency. In addition, our study also shows that genetic interaction of Cited2 with HIF-1 signaling contributes to the appropriate formation of the hyaloid vascular system (HVS) during development.

MATERIALS AND METHODS

Mouse lines and preparation of mouse embryos

Cited2$^{+/-}$ (Yin et al., 2002) and *Cited2*$^{flox/flox}$ (Preis et al., 2006) mouse lines were maintained on the C57BL/6 background. *Cited2*$^{flox/flox}$ mice were mated with *Le-Cre*$^{+}$ mice to generate *Cited2*$^{flox/flox}$;*Le-Cre*$^{-}$ and *Cited2*$^{flox/flox}$;*Le-Cre*$^{+}$ mice. *Hif1a*$^{flox/flox}$ (Cramer et al., 2003);*Le-Cre*$^{+}$ (Ashery-Padan et al., 2000) mice were mated with *Cited2*$^{+/-}$ mice to generate embryos with the following genotypes: *Cited2*$^{-/-}$;*Hif1a*$^{flox/flox}$;*Le-Cre*$^{+}$,

Cited2$^{-/-}$;*Hif1a*$^{flox/flox}$;*Le-Cre*$^{-}$, *Cited2*$^{+/+}$;*Hif1a*$^{flox/flox}$;*Le-Cre*$^{+}$, *Cited2*$^{+/+}$;*Hif1a*$^{flox/flox}$;*Le-Cre*$^{-}$, *Cited2*$^{+/-}$; *Hif1a*$^{flox/flox}$;*Le-Cre*$^{+}$, or *Cited2*$^{+/-}$;*Hif1a*$^{flox/flox}$;*Le-Cre*$^{-}$. Primers for genotyping were: HIF-1α-flox: antisense (a), 5′-ATATGCTCTTATGAAGGGGCCTATGGAGGC-3′ and sense (s), 5′-GATCTTTCCGAGGACCTGGATTCAATTCCC-3′; Le-Cre (a), 5′-GCATTACCGGTCGATGCAACGAGTGATGAG-3′ and (s), 5′-GAGTGAACGAACCTGGTCGAAATCAGTGCG-3′. PAX77 transgenic mice overexpressing the human *PAX6* gene (Schedl et al., 1996) were mated with *Cited2*$^{+/-}$ mice to produce *Cited2*$^{+/-}$ mice carrying the *PAX6* transgene. These compound mice were then mated with *Cited2*$^{+/-}$ mice to obtain *Cited2*$^{-/-}$ embryos with and without the transgene at 14.5 dpc. PAX77 transgenic mice were genotyped as described previously (Kleinjan et al., 2006). All animal husbandry and experiments were conducted in accordance with institutional guidelines of Case Western Reserve University. Timed pregnancy of *Cited2*$^{+/-}$ females was determined as 0.5 dpc if vaginal plug was found after overnight mating. Embryos were harvested by a caesarean-driven method.

Histology

Embryos at 10.5, 11.5, 12.5, 13.5, 15.5 and 18.5 dpc were fixed in 10% formalin, dehydrated, embedded in paraffin and processed with 7 μm transverse sectioning. Histology of the eyes was examined by light microscopy after Hematoxylin and Eosin staining.

Immunohistochemistry and X-Gal staining for eye sections

For immunohistochemistry, embryonic tissues were fixed in 1-4% paraformaldehyde, equilibrated in 12%, 15% and 20% sucrose, embedded in OCT and processed with 10 μm cryosectioning. Immunostaining employed antibodies against Cited2 (Santa Cruz), E-cadherin (cadherin 1) (BD Pharmingen) and α smooth muscle actin (α-SMA) (Sigma) and antibody staining was visualized with Alexa594-conjugated anti-mouse secondary antibody (Molecular Probes, Invitrogen). Phosphorylated histone H3 immunostaining was performed with anti-phospho-H3 antibody (Cell Signaling) and the staining was visualized with Alexa488-conjugated anti-rabbit secondary antibody (Molecular Probes, Invitrogen). Antibodies against CD31 (Pecam1 – Mouse Genome Informatics) (BD Pharmingen) and VEGFR2 (Flk1; Kdr) (BD Pharmingen) were visualized with 3,3′-diaminobenzidine (Sigma). Pax6 and AP2α antibodies were obtained from Developmental Studies Hybridoma Bank at University of Iowa and the staining was visualized by Alexa594-conjugated anti-mouse secondary antibody and 3,3′-diaminobenzidine, respectively. *lacZ* expression was detected by X-Gal (Roche) staining and was performed on 1% paraformaldehyde-fixed eye sections according to standard methods.

TUNEL assay

Cryosections were collected from 10.5 dpc embryos after fixation in 4% paraformaldehyde and processed for the TUNEL assay according to the manufacturer's instruction (Chemicon).

Real-time RT-PCR

Total RNA was extracted using RNA Trizol (Invitrogen) and was reverse transcribed into cDNA using the SuperScript First-Strand Synthesis System for RT-PCR Kit (Invitrogen). PCR primers for detecting *Pax6* expression in *Cited2*$^{-/-}$ and *Cited2*$^{+/+}$ embryonic lens were: antisense (a), 5′-CTACCAGCCAATCCCACAGC-3′ and sense (s), 5′-TTCGGCCCAACATGGAAC-3′. Primers for detecting *Pax6* expression in lenses collected from *Cited2*$^{-/-}$;PAX77 and *Cited2*$^{-/-}$ littermate control embryos were: (a), 5′-ATGTTGCGGAGTGATTAGTGGG-3′ and (s), 5′-GCGAAGCCTGACCTCTGTCA-3′. *Vegf* (*Vegfa* – Mouse Genome Informatics) and *Hif1a* mRNA expression was analyzed as

described previously (Xu et al., 2007). The real-time PCR was performed in triplicate for each sample on MyiQ (BioRad). Ct value was recorded to perform data analysis.

Luciferase assay

α-TN4-1, NMuMG and HEK293 cells were seeded in 12-well plates for transfection of 0.15 ng pRLSV40, 270 ng of LE9-P0, LE0-P0 or P0 firefly luciferase reporter, various amounts of Cited2 expression plasmid, 75 ng of Pax6 expression plasmid, and control plasmid so that the total amount of DNA was 1 μg/well. Fugene6 transfection reagent (Roche) was used for the transfection. Firefly and *Renilla* luciferase activities were measured 24 hours after transfection using Dual-Luciferase Assay Reagents (Promega) on a luminometer. Relative luciferase activity was calculated by dividing firefly luciferase activity by *Renilla* luciferase activity.

Chromatin immunoprecipitation

Chromatin immunoprecipitation (ChIP) was performed in α-TN4-1 cells according to protocols previously described (Yang and Cvekl, 2005; Yang et al., 2006) using antibodies against Cited2 and Pax6 (Santa Cruz). The immunoprecipitated DNAs were amplified by PCR and analyzed by agarose gel electrophoresis. Primers for the ChIP assay spanning the *Pax6* LE9 region and the *Pax6* P0 promoter region were: LE9 region (a), 5′-TGGGCAATGAGCGGAAAGAT-3′ and (s), 5′-TGTGTGCAAATGAAGGCTCTCC-3′; P0 region (a), 5′-CGAGGGTGGGGTGTCAGGTG-3′ and (s), 5′-GCGGCTTTGAGAAGTGTGGG-3′. Another pair of primers covering the region between LE9 and the P0 promoter was chosen as a negative control (NC): (a), 5′-TCAAGGAACATCTGGCTCGC-3′ and (s), 5′-GATGGGGCTCCACCAATCCA-3′.

RESULTS

Expression of Cited2 in the developing lens

Expression of Cited2 in the developing lens was examined by immunostaining of embryonic eye sections. Cited2 expression was detected in the surface ectoderm at 9.5 dpc (Fig. 1A,E), in the invaginating lens pit at 10.5 dpc (Fig. 1B,F), and in lens epithelial cells at later stages such as 15.5 dpc (Fig. 1C,G). The expression of Cited2 was not detected in differentiated lens fiber cells during lens development (Fig. 1C,G). The expression of Cited2 in the developing lens suggests its potential involvement in lens morphogenesis. In addition to the lens, Cited2 was also expressed in the other developing ocular components, such as the cornea, the non-pigmented layer of the ciliary epithelium and retina (Fig. 1C,G).

Abnormal corneal-lenticular stalk formation in *Cited2*$^{-/-}$ developing eyes

Gross morphological examination revealed several prominent abnormalities with full penetrance in all the *Cited2*$^{-/-}$ eyes examined (Table 1). In the anterior part of *Cited2*$^{-/-}$ eyes, abnormal corneal-lenticular stalk formation was consistently observed, which resembles Peters' anomaly, a congenital defect with persistent central adhesion between the lens and the cornea (Yoon, 2001;Smith and Velzeboer, 1975;Myles et al., 1992;Kenyon, 1975). In contrast to wild-type littermate controls (Fig. 2A,C,E), *Cited2*$^{-/-}$ lens vesicles failed to separate from the surface ectoderm at 11.5 dpc (Fig. 2B), resulting in a persistent corneal-lenticular stalk as shown by representative pictures from 15.5 dpc (Fig. 2D) and 18.5 dpc (Fig. 2F). The corneal-lenticular stalk was further examined by immunostaining of E-cadherin. Abnormal corneal-lenticular stalk in *Cited2*$^{-/-}$ eyes (Fig. 2H), which was absent from the wild-type control (Fig. 2G), was positively stained for E-cadherin, validating the epithelial characteristics of the corneal-lenticular stalk. In addition, a distinctive endothelial layer on the posterior side of the cornea developed in wild-type eyes by 15.5 dpc (see Fig. S1A in the supplementary material), whereas it was absent in *Cited2*$^{-/-}$ eyes (see Fig. S1B in the supplementary material).

Cited2$^{-/-}$ developing lenses were also smaller than in the wild type. Decreased lens size was first noted as early as 10.5 dpc in *Cited2*$^{-/-}$ embryos as smaller invaginating lens placodes (see Fig. S2B in the supplementary material) than in wild-type littermate controls (see Fig. S2A in the supplementary material). Smaller lens vesicles were thus formed in the developing *Cited2*$^{-/-}$ eyes at 11.5 dpc as shown above (Fig. 2B), and the *Cited2*$^{-/-}$ lenses remained small throughout the subsequent stages until 18.5 dpc (see Fig. S2D in the supplementary material), as compared with wild-type littermate controls (see Fig. S2C in the supplementary material). Retinal folding was also invariably detected in *Cited2*$^{-/-}$ eyes at 18.5 dpc (see Fig. S2D in the supplementary material), which might, in part, result from abnormal lens formation (Chow and Lang, 2001).

Proliferation and cell death rate in early *Cited2*$^{-/-}$ developing lens

To further explore the mechanisms responsible for small lens size in *Cited2*$^{-/-}$ eyes, proliferation of the lens cells was examined by the expression of a mitosis marker, phosphorylated histone H3, in the developing lens at 10.5 dpc. As shown in Fig. 3, no significant difference in mitosis was revealed when *Cited2*$^{-/-}$ lens (n=5) (Fig. 3B) was compared with *Cited2*$^{+/+}$ littermate controls (n=3) (Fig. 3A) [14.3±1% in *Cited2*$^{+/+}$ versus 12.5 ±1.6% in *Cited2*$^{-/-}$ lens, P>0.05 (Fig. 3C)]. Cell death in the developing lens at 10.5 dpc was also examined in parallel by the TUNEL assay. Compared with the *Cited2*$^{+/+}$ littermate controls (n=3) (Fig. 3D), increased cell death was detected in the *Cited2*$^{-/-}$ lens (n=5) (Fig. 3E) [13.5 ±1.8% in *Cited2*$^{+/+}$ versus 25.1±5.4% in the *Cited2*$^{-/-}$ lens, P<0.01 (Fig. 3F)]. Collectively, Cited2 deficiency may result in increased cell death during early lens development, which in turn may contribute to the smaller lens size at subsequent developmental stages.

Aberrant vitreous hypercellularity consisting of aberrant vascularization in *Cited2*$^{-/-}$ developing eyes

In the posterior part of *Cited2*$^{-/-}$ eyes, hypercellularity of the hyaloid vasculature was observed. Fig. 4 shows representative pictures of *Cited2*$^{-/-}$ eyes from 15.5 (Fig. 4B) and 18.5 dpc (Fig. 4D) and wild-type littermate controls from corresponding stages (Fig. 4A,C). Further immunohistochemical examination for vasculature was performed with antibodies against CD31, a molecular marker for vascular endothelial cells, and vascular endothelial growth factor (VEGF) receptor 2 (VEGFR2), which is expressed by angioblast cells and vascular endothelial cells (Ash and Overbeek, 2000). In wild-type littermate controls at 15.5 dpc, CD31 (Fig. 4E) and VEGFR2 expression (Fig. 4G) was detected in pupillary membrane vessels, tunica vasculosa lentis and vasculature overlying the developing retina. However, *Cited2*$^{-/-}$ eyes were predominantly featured by excessive and disorganized vasculature in the developing vitreous that was positive for expression CD31 (Fig. 4F) and VEGFR2 (Fig. 4H).

Cited2 is required for the regression of the hyaloid vascular system through modulating HIF-1 signaling during eye development

Angiogenic factor VEGF is expressed in different components of the developing eye, including the lens, the cornea and the retina, suggesting that VEGF might be one of the growth factors that initiate intraocular angiogenesis (Flamme et al., 1995). Overproduction of VEGF in the lens results in excessive accumulation of angioblasts and endothelial cells, indicating that the expression level of VEGF in the lens is critical for the maturation of the HVS (Ash and Overbeek, 2000; Mitchell et al., 2006; Rutland et al., 2007). VEGF is a direct target of HIF-1 (Liu et al., 1995; Shweiki et al., 1992) and, importantly, Cited2 has been shown to be a negative regulator for HIF-1 signaling through its competitive binding to the CH1 domain of CBP/p300 with higher affinity than does HIF-1α (Bhattacharya et al., 1999). In Cited2-deficient mouse heart, HIF-1 signaling is deregulated, as evidenced by increased expression of HIF-1-inducible genes, including *Vegf* (Yin et al., 2002). HIF-1α haploinsufficiency decreases VEGF

expression and rescues the heart defects in Cited2-deficient embryos (Xu et al., 2007), indicating that upregulated HIF-1 signaling is in part responsible for defective cardiac morphogenesis resulting from Cited2 deficiency. Altered expression of VEGF as a result of upregulated HIF-1 signaling is of significance considering the role of VEGF in the hyaloid vascularization. Interestingly, a 4.5-fold increase in the *Vegf* mRNA level was detected in *Cited2*$^{-/-}$ lens compared with the wild-type littermate control (Fig. 4I), suggesting that upregulated HIF-1 signaling as a result of Cited2 deficiency could be responsible for the elevated VEGF expression and hyaloid hypercellularity and aberrant vascularization in *Cited2*$^{-/-}$ eyes. We tested this hypothesis by introducing Le-Cre (Ashery-Padan et al., 2000) mediated lens-specific deletion of *Hif1a* in Cited2-deficient eyes. *Cited2*$^{-/-}$;*Hif1a*$^{flox/flox}$;*Le-Cre*$^{-}$ eyes reproducibly displayed the persistence of lens stalk and hyaloid hypercellularity with aberrant vasculature at 15.5 (Fig. 5A) and 17.5 dpc (Fig. 5C) (n=3), which contrasted with the normal littermate control at 15.5 dpc (see Fig. S3A,B in the supplementary material) and 17.5 dpc (see Fig. S3C,D in the supplementary material) (n=2). Furthermore, compared with *Cited2*$^{-/-}$;*Hif1a*$^{flox/flox}$;*Le-Cre*$^{-}$ eyes, hyaloid hypercellularity with aberrant vasculature was not detected in *Cited2*$^{-/-}$;*Hif1a*$^{flox/flox}$;*Le-Cre*$^{+}$ eyes from the same litters at the corresponding stages; however, the corneal-lenticular stalk was still present in these eyes (n=3) (Fig. 5B,D). The efficiency of *Le-Cre* transgene-mediated deletion of *Hif1a* in *Cited2*$^{-/-}$ eyes was also assessed by analyzing *Hif1a* mRNA expression in the lens at 14.5 dpc. The result showed a 5-fold reduction of *Hif1a* mRNA expression in *Cited2*$^{-/-}$;*Hif1a*$^{flox/flox}$;*Le-Cre*$^{+}$ lens (n=3) compared with that in *Cited2*$^{-/-}$;*Hif1a*$^{flox/flox}$;*Le-Cre*$^{-}$ littermate controls (n=3) (Fig. 5E). Furthermore, there was a 3-fold reduction in the *Vegf* mRNA level in *Cited2*$^{-/-}$;*Hif1a*$^{flox/flox}$;*Le-Cre*$^{+}$ lens (n=3) compared with *Cited2*$^{-/-}$;*Hif1a*$^{flox/flox}$;*Le-Cre*$^{-}$ littermate controls (n=4) (Fig. 5F). Thus, our results support the hypothesis that upregulated HIF-1 signaling as a result of Cited2 deficiency is indeed responsible for the aberrant vitreous hypercellularity and disorganized hyaloid vasculature, as deletion of *Hif1a* in the lens can specifically rescue this phenotype in Cited2-deficient eyes.

Cited2 positively regulates Pax6 expression in the lens

Transcription factor Pax6 is a highly conserved master regulator for eye development (Grindley et al., 1995; Chow and Lang, 2001) and *Pax6* gene dosage exerts a critical influence on lens morphogenesis. Haploinsufficiency of Pax6 results in abnormal lens morphogenesis highlighted by corneal-lenticular stalk formation (Dimanlig et al., 2001; Davis-Silberman et al., 2005), which shares striking similarities with the corneal-lenticular stalk phenotype observed in *Cited2*$^{-/-}$ eyes. Moreover, the expression of Cited2 in lens epithelial cells overlaps with that of Pax6 in the developing eye (Grindley et al., 1995; Walther and Gruss, 1991). We thus hypothesized that Cited2 might affect the level of Pax6 expression in developing lens and that decreased Pax6 expression in Cited2-deficient eyes might lead to corneal-lenticular stalk formation. To explore this possibility, immunostaining of Pax6 was performed. An appreciable level of Pax6 expression in *Cited2*$^{-/-}$ lens epithelial cells was detected at 13.5 dpc (Fig. 6B) as compared with the wild-type littermate control (Fig. 6A). Since a quantitative comparison of Pax6 expression levels was hard to achieve by immunostaining, we compared mRNA expression of *Pax6* in wild-type and Cited2-deficient lens at 14.5 dpc by real-time PCR. We observed a 2.5-fold reduction in *Pax6* mRNA expression in *Cited2*$^{-/-}$ lens (n=4) as compared with wild-type littermate controls (n=4) (Fig. 6C).

Pax6 expression in the lens is regulated through a series of cis-regulatory elements in addition to its promoter for correct spatiotemporal and quantitative expression (Xu et al., 1999; Kammandel et al., 1999; Kleinjan et al., 2006). Transgenic studies in conjunction with gene-targeting strategy and in vitro studies have established that the head surface ectoderm enhancer is one of the major regulators for Pax6 expression in the lens (Kammandel et al., 1999). Disruption of the ectoderm enhancer causes lens defects including small lens and fusion of the

lens to the surface ectoderm (Dimanlig et al., 2001). In vitro studies have identified a Pax6-responsive element in the ectoderm enhancer and established a model in which Pax6 protein regulates its own expression through a direct interaction of Pax6 with the surface ectoderm enhancer (Aota et al., 2003). To further examine the potential involvement of Cited2 in regulating Pax6 expression, reporter constructs containing the *Pax6* promoter (P0) and two enhancer fragments, LE9 (LE9-P0) and LE0 (LE0-P0) (Aota et al., 2003), responsible for autoregulated expression of Pax6, were tested in a lens epithelial cell line, α-TN4-1, which expresses a high endogenous level of Pax6 (Yang and Cvekl, 2005), and in a normal mouse mammary gland epithelial cell line, NMuMG, which does not express Pax6. In α-TN4-1 cells, Cited2 overexpression significantly increased LE9-P0 reporter activity (Fig. 6D,E) in a dose-dependent manner (data not shown). In addition, LE0-P0 and P0 reporter activity was enhanced when Cited2 was overexpressed (Fig. 6D). However, in NMuMG cells in which Pax6 is absent, Cited2 expression had no effect on the LE9-P0 reporter activity. When Cited2 was co-expressed with Pax6 in NMuMG cells, the reporter activity was significantly increased as compared with Pax6 alone (Fig. 6E). Similar data were obtained in human embryonic kidney (HEK293) cells (Fig. 6E). Chromatin immunoprecipitation (ChIP) was then carried out to test whether Cited2 is physically present on the *Pax6* ectoderm enhancer and the P0 promoter region using chromatin prepared from α-TN4-1 cells. The results showed that Cited2 is present on the genomic region covering the LE9 sequence and the *Pax6* P0 promoter (Fig. 6Fa,b), but absent in other regions upstream of the *Pax6* P0 promoter (Fig. 6Fc). This is consistent with the transfection results (Fig. 6D) and the previous finding that Pax6 binds the LE9 enhancer and the P0 promoter of the *Pax6* gene (Aota et al., 2003). These data strongly suggest that Cited2 is a potential positive regulator for Pax6 expression in the lens.

To definitively demonstrate that Cited2 is a positive regulator of Pax6 in vivo, we generated compound embryos by crossing the *PAX6* transgenic mouse line (Schedl et al., 1996) onto a *Cited2* knockout background to test whether the Cited2-deficient lens phenotype could be rescued by increasing *Pax6* gene dosage. As shown in Fig. 6E, *Cited2*$^{-/-}$;*Pax6*$^{-}$ mouse embryos reproducibly displayed corneal-lenticular stalk formation (*n*=2) (Fig. 6G), whereas the abnormal corneal-lenticular stalk was never detected in any of the *Cited2*$^{-/-}$;*Pax6*$^{+}$ embryos analyzed (*n*=3) (Fig. 6H). Quantitative analysis revealed a 2.3-fold increase of *Pax6* mRNA expression in *Cited2*$^{-/-}$;*Pax6*$^{+}$; mouse lens (*n*=3) as compared with that from *Cited2*$^{-/-}$;*Pax6*$^{-}$ littermate controls (*n*=3) (data not shown). Our data thus indicate that increased Pax6 expression in Cited2-deficient embryos is able to correct abnormal corneal-lenticular stalk formation. These data provide direct evidence that decreased Pax6 expression is indeed responsible for the corneal-lenticular stalk formation in Cited2-deficient embryos. Therefore, Cited2 is essential for lens morphogenesis by functioning upstream of, and/or together with, Pax6, as the latter increases its own expression. Taken together, our in vitro and in vivo data demonstrate that Cited2 is a novel regulator for Pax6 expression in the lens.

Cited2 is required for lens morphogenesis and proper regression of HVS

Since targeted deletion of *Cited2* is embryonic lethal, to further address the role of Cited2 in lens morphogenesis and HVS formation and regression in adult mice, lens-specific deletion of *Cited2* was generated by crossing *Cited2*$^{flox/flox}$ mice with *Le-Cre* transgenic mice. It is worth noting that the construct strategy allows *lacZ* to be expressed under the control of the *Cited2* promoter when the floxed *Cited2* allele is recombined (Preis et al., 2006). Therefore, we could assess the *Le-Cre* transgene-mediated recombination of floxed *Cited2* alleles by X-Gal staining. As shown in Fig. 7, *lacZ* expression was readily detected in *Cited2*$^{flox/flox}$;*Le-Cre*$^{+}$ eyes during early lens development, including lens placode at 9.5 dpc (Fig. 7A), invaginating lens pit at 10.5 dpc (Fig. 7B) and lens vesicle at 11.5 dpc (Fig. 7C), whereas no *lacZ* staining was detected in *Cited2*$^{flox/flox}$;*Le-Cre*$^{-}$control eyes (Fig. 7D). Additionally, failed separation of the lens from the surface ectoderm at 11.5 dpc was recapitulated in the *Cited2*$^{flox/flox}$;*Le-*

Cre^{+} eye (Fig. 7C), as was shown in *Cited2*$^{-/-}$eyes at the same developmental stage (Fig. 2B). These results indicate that (1) the *Le-Cre* transgene mediates successful deletion of *Cited2* in the developing lens and (2) the *Le-Cre* transgene is active in developing lens starting from the lens placode stage, which is consistent with what was reported previously (Ashery-Padan et al., 2000).

Moreover, morphological examination revealed that compared with the *Cited2*$^{flox/flox}$;*Le-Cre*$^{-}$ littermate control at 6 weeks of age (Fig. 7E), the *Cited2*$^{flox/flox}$;*Le-Cre*$^{+}$ eye was smaller and displayed failed formation of the anterior chamber (Fig. 7F). This was further supported by histological analysis, which showed failed separation of the lens from the cornea and defective anterior chamber formation (Fig. 7H) as compared with the normal histological feature exhibited by the *Cited2*$^{flox/flox}$;*Le-Cre*$^{-}$littermate control (Fig. 7G). In addition, abnormal retrolental tissue was invariably noted in *Cited2*$^{flox/flox}$;*Le-Cre*$^{+}$ eyes (Fig. 7J) compared with the *Cited2*$^{flox/flox}$;*Le-Cre*$^{-}$ littermate control (Fig. 7I). Higher magnification revealed that the retrolental mass consists of melanocytes and blood vessels (Fig. 7K), and the latter was confirmed by immunostaining for α smooth muscle actin, which labels the pericytes that stabilize the vessels (Fig. 7L). These results indicate that Cited2 is required for lens morphogenesis and that Cited2 deficiency is associated with abnormal HVS regression in the eye.

DISCUSSION

The current study is the first evaluation of the role of Cited2 in eye morphogenesis. Our results show that Cited2 is expressed in the developing eye and that deletion of *Cited2* disturbs normal eye development, causing fusion of the lens to the cornea and hyaloid hypervascularity. Genetic interaction of Cited2 with HIF-1 signaling is specifically involved in the process of HVS formation. In addition, Cited2 functions upstream of, and/or together with, Pax6, a key transcription factor in lens morphogenesis.

Function of Cited2 in regulating the fetal vasculature

Fetal hyaloid vasculature is required to provide nutrients to various compartments of the developing eye. However, the hyaloid vasculature is a transient blood supply system in that a gradual loss followed by a nearly complete regression is achieved during postnatal ocular development in mammals (Ito and Yoshioka, 1999). Abnormalities in the process of intraocular vascularization during embryogenesis are linked to several disorders, including Persistent fetal vasculature (PFV) with vision impairment (Pollard, 1997; Haddad et al., 1978; Goldberg, 1997). The mechanisms responsible for the fetal hyaloid vasculogenesis and subsequent regression have not been clearly defined.

Our current study provides evidence that Cited2-HIF-1 genetic interaction plays an important role in this process. HIF-1 signaling is the major machinery that responds to low oxygen level in various tissue types. Under hypoxic condition, HIF-1α, the subunit of HIF-1 whose expression is controlled by oxygen levels, accumulates, binds with its heterodimeric partner, HIF-1β, translocates to the nucleus, binds to hypoxia-response elements and recruits p300 via the CH1 domain, thus activating the transcription of its target genes, including *Vegf* (Pugh and Ratcliffe, 2003; Arany et al., 1996). *Cited2* is a hypoxia-inducible gene that modulates HIF-1 signaling by binding p300 with higher affinity than does HIF-1α. This competitive binding reduces hypoxia-activated transcription (Freedman et al., 2003; Bhattacharya et al., 1999). Therefore, as a negative regulator for HIF-1 signaling, Cited2 plays an important role in controlling the HIF-1α-mediated hypoxia response. Our previous studies have shown that in *Cited2*$^{-/-}$ mouse hearts, HIF-1 signaling is upregulated, as measured by increased expression of HIF-1 target genes, including *Vegf* (Yin et al., 2002). Furthermore, HIF-1α haploinsufficiency partially rescues heart morphogenic phenotypes, providing evidence that

Cited2 deficiency causes deregulated HIF-1 signaling under hypoxic conditions and that the latter is partially responsible for the heart malformations in *Cited2*$^{-/-}$embryos (Xu et al., 2007).

The lens exists in a hypoxic environment (Bassnett and McNulty, 2003; Shui et al., 2003; Shui et al., 2006). The role of VEGF in intraocular vascularization has been studied extensively. Preliminary reports suggest that deletion of VEGF in the lens prevents the formation of the capillary network on the posterior of the lens without disturbing lens formation or the establishment of hyaloid vasculature (Beebe, 2008). By contrast, increased expression of VEGF in the lens invariably leads to the production of excess, aberrant hyaloid vascularization (Ash and Overbeek, 2000; Mitchell et al., 2006; Rutland et al., 2007). Based on these findings and the data presented in this work, increased VEGF levels resulting from deregulated Cited2-HIF-1 could be considered as one of the factors involved in aberrant hyaloid vascularization in *Cited2*$^{-/-}$ eyes. However, our results do not exclude the possibility that other mechanisms might also be involved. Specific deletion of *Vegf* in *Cited2*$^{-/-}$ lens will help to clarify the role of Cited2-HIF-1 interaction in the control of lenticular VEGF production during eye development and the participation of other growth factors in the process. Since mutants that form smaller lenses often have more mesenchyme in the vitreous (Beebe et al., 2004), it is possible that the smaller lens resulting from deletion of *Cited2* might allow more mesenchymal cells to migrate into the developing vitreous, directly or indirectly promoting the formation of an increased vascular supply. Alternatively, lower levels of anti-angiogenic factors could be produced by the mutant lens, which might perturb the necessary balance between angiogenic and anti-angiogenic factors during HVS development.

Since HIF-1 signaling is also involved in regulating cell death and proliferation (Carmeliet et al., 1998), it might control the size of the lens through these mechanisms and, in turn, affect hyaloid vascularization. Our preliminary data showed that Cited2-deficient lens appeared to have increased levels of apoptotic cells at 10.5 dpc, which was only partially corrected by deleting *Hif1a* in Cited2-deficient eyes (data not shown). Proliferation assays did not reveal any obvious changes in Cited2-deficient embryos compared with their wild-type littermate controls. This is consistent with the conclusion that HIF-1 is not the decisive factor controlling lens growth in younger animals (Beebe, 2008). Further analysis will be required to define the relative contributions of lens size, VEGF expression, hyaloid vascularization and migration of mesenchymal cells to the formation of the HVS. Conditional deletion of both *Cited2* and *Hif1a* might further clarify whether Cited2-HIF-1α interaction contributes to the regression of the HVS postnatally.

Function of Cited2 in lens morphogenesis

Our data have shown that the formation of a corneal-lenticular stalk in *Cited2*$^{-/-}$ eyes is mediated by mechanisms independent of HIF-1, as lens-specific deletion of *Hif1a* did not rescue this defect. Pax6 is a key regulator for various eye developmental events including lens morphogenesis (Hill et al., 1991; Hanson et al., 1994; Kaufman et al., 1995; Quiring et al., 1994). *Pax6* gene dosage is critical for lens morphogenesis, which is supported by independent studies from *Sey* heterozygous mice (van Raamsdonk and Tilghman, 2000; Hill et al., 1991), *Pax6* head surface ectoderm enhancer null mice (Dimanlig et al., 2001) and *Pax6* single allele knockout mice (Davis-Silberman et al., 2005). For example, *Pax6* single allele deletion in the lens results in a 34% reduction in the Pax6 level in *Pax6*$^{flox/+}$;*Le-Cre*$^{+}$ mouse lens epithelium, which is sufficient to cause corneal-lenticular stalk formation in the eye (Davis-Silberman et al., 2005). In human, heterozygous *PAX6* mutations are associated with Peters' anomaly (Hanson et al., 1994; Smith and Velzeboer, 1975; Myles et al., 1992; Kenyon, 1975), in which the patients are characterized by fusion of the lens to the cornea. Owing to its gene dosage effect on lens morphogenesis, transcriptional control of *Pax6* gene expression has been the

subject of a number of studies, which have identified a series of cis-regulatory elements upstream of *Pax6*, within the introns of *Pax6*, downstream of *Pax6* or within the introns of an adjacent gene (Williams et al., 1998; Xu et al., 1999; Kammandel et al., 1999; Kleinjan et al., 2001; Kleinjan et al., 2002; Kleinjan et al., 2006). Cited2 deficiency resulted in corneal-lenticular stalk formation and decreased Pax6 expression, suggesting that Cited2 might control Pax6 expression. Our in vitro data also suggested that Cited2 could be a positive regulator for Pax6 autoregulation. In vivo data from *Cited2*$^{-/-}$;*Pax6*$^{+}$ mouse embryonic eyes showed that increasing *Pax6* gene dosage in *Cited2*$^{-/-}$ eyes corrected the corneal-lenticular stalk phenotype, providing direct genetic evidence that Cited2 is required for normal levels of Pax6 expression in the lens. Although we found that Cited2 regulated Pax6 expression through its action on regions within the upstream head surface ectoderm enhancer and the P0 promoter, we cannot exclude the possible involvement of downstream regulatory elements (Kleinjan et al., 2006) in Cited2-mediated expression of Pax6. Further studies are necessary to determine how Cited2 interacts with these cis elements to control Pax6 expression. Additionally, although a direct physical interaction between Pax6 and Cited2 was not detected by co-immunoprecipitation after overexpressing Pax6 and Cited2 in HEK293 cells (data not shown), it is possible that Cited2, Pax6 and other proteins, such as Sox2 (Aota et al., 2003) and Oct1 (Pou2f1 – Mouse Genome Informatics) (Donner et al., 2007), are present in a multi-protein complex. Biochemical characterization of this multi-protein complex will be necessary to provide a molecular basis for Cited2 involvement in the autoregulation of Pax6 expression. It is also worth noting that although Cited2 activates *Pax6* upstream regulatory elements in vitro (Fig. 6D), Cited2 might not be the only molecule controlling Pax6 expression in the developing lens. This is in part supported by the observation that *Cited2* homozygous deletion only results in a 2.5-fold reduction of the *Pax6* mRNA level in the developing lens (Fig. 6C). In addition, the *Le-Cre* transgene driven by the *Pax6* upstream ectoderm enhancer and the P0 promoter in the *Cited2*-null background efficiently deletes floxed *Hif1a* (Fig. 5), suggesting that other factors might also contribute to the transcriptional activity of the *Pax6* upstream ectoderm enhancer and P0 promoter.

Although we have provided experimental evidence that Cited2 plays important roles in lens morphogenesis in part through regulating Pax6 expression in the developing lens, other mechanisms, involving, for example, AP2α cannot be ruled out at the present time. Cited2 and AP2α physically interact to impact cardiac morphogenesis, left-right patterning and neural tube formation (Bamforth et al., 2001; Bamforth et al., 2004). *Ap2a*-null mice display eye developmental defects, such as corneal-lenticular adhesion, demonstrating that AP2α is required for lens development (West-Mays et al., 1999). We detected appreciable level of AP2α in *Cited2*$^{-/-}$ lens epithelial cells (see Fig. S4B in the supplementary material) as compared with wild-type littermate controls (see Fig. S4A in the supplementary material). Cited2 could function as a co-activator of AP2α to regulate the expression of its as-yet-unidentified target genes, which in turn would contribute to the lens phenotypes observed in *Cited2*$^{-/-}$eyes.

As a transcriptional modulator, Cited2 has been shown to be involved in the development of several organs and tissues. However, the role of Cited2 in eye development has not been explored previously. The current study has uncovered a novel function of Cited2 in lens morphogenesis and hyaloid vascular development, and offers mechanistic views of how Cited2 functions in these processes. This information might shed new light on the etiology of, and potential therapeutic strategies for, eye disorders such as Peters' anomaly and PFV.

Supplementary Material

Refer to Web version on PubMed Central for supplementary material.

Acknowledgements

We thank Drs John Ash, Paul Overbeek and Joe Hollyfield for insightful discussion and suggestions; Dr Hisato Kondoh for plasmids for in situ hybridization; Dr Ying Yang for the ChIP assay protocol; Drs Yoshikazu Imanishi and Tadao Maeda for the retinal FITC-dextran perfusion experiment; and Eric Lam for technical assistance. This research was supported by National Institutes of Health grants R01-HL075436 (Y.C.Y. and M.W.) and R01-HL076919 (Y.-C.Y.). S.L.D. is a Pfizer Foundation Australia Senior Research Fellow.

References

Aota S, Nakajima N, Sakamoto R, Watanabe S, Ibaraki N, Okazaki K. Pax6 autoregulation mediated by direct interaction of Pax6 protein with the head surface ectoderm-specific enhancer of the mouse Pax6 gene. Dev Biol 2003;257:1–13. [PubMed: 12710953]

Arany Z, Huang LE, Eckner R, Bhattacharya S, Jiang C, Goldberg MA, Bunn HF, Livingston DM. An essential role for p300/CBP in the cellular response to hypoxia. Proc Natl Acad Sci USA 1996;93:12969–12973. [PubMed: 8917528]

Ash JD, Overbeek PA. Lens-specific VEGF-A expression induces angioblast migration and proliferation and stimulates angiogenic remodeling. Dev Biol 2000;223:383–398. [PubMed: 10882523]

Ashery-Padan R, Marquardt T, Zhou X, Gruss P. Pax6 activity in the lens primordium is required for lens formation and for correct placement of a single retina in the eye. Genes Dev 2000;14:2701–2711. [PubMed: 11069887]

Bamforth SD, Braganca J, Eloranta JJ, Murdoch JN, Marques FI, Kranc KR, Farza H, Henderson DJ, Hurst HC, Bhattacharya S. Cardiac malformations, adrenal agenesis, neural crest defects and exencephaly in mice lacking Cited2, a new Tfap2 co-activator. Nat Genet 2001;29:469–474. [PubMed: 11694877]

Bamforth SD, Braganca J, Farthing CR, Schneider JE, Broadbent C, Michell AC, Clarke K, Neubauer S, Norris D, Brown NA, et al. Cited2 controls left-right patterning and heart development through a Nodal-Pitx2c pathway. Nat Genet 2004;36:1189–1196. [PubMed: 15475956]

Barbera JP, Rodriguez TA, Greene ND, Weninger WJ, Simeone A, Copp AJ, Beddington RS, Dunwoodie S. Folic acid prevents exencephaly in Cited2 deficient mice. Hum Mol Genet 2002;11:283–293. [PubMed: 11823447]

Bassnett S, McNulty R. The effect of elevated intraocular oxygen on organelle degradation in the embryonic chicken lens. J Exp Biol 2003;206:4353–4361. [PubMed: 14581604]

Beebe D, Garcia C, Wang X, Rajagopal R, Feldmeier M, Kim JY, Chytil A, Moses H, Ashery-Padan R, Rauchman M. Contributions by members of the TGFbeta superfamily to lens development. Int J Dev Biol 2004;48:845–856. [PubMed: 15558476]

Beebe DC. Maintaining transparency: A review of the developmental physiology and pathophysiology of two avascular tissues. Semin Cell Dev Biol 2008;19:125–133. [PubMed: 17920963]

Bhattacharya S, Michels CL, Leung MK, Arany ZP, Kung AL, Livingston DM. Functional role of p35srj, a novel p300/CBP binding protein, during transactivation by HIF-1. Genes Dev 1999;13:64–75. [PubMed: 9887100]

Carmeliet P, Dor Y, Herbert JM, Fukumura D, Brusselmans K, Dewerchin M, Neeman M, Bono F, Abramovitch R, Maxwell P, et al. Role of HIF-1[alpha] in hypoxia-mediated apoptosis, cell proliferation and tumour angiogenesis. Nature 1998;394:485–490. [PubMed: 9697772]

Chen Y, Haviernik P, Bunting KD, Yang YC. Cited2 is required for normal hematopoiesis in the murine fetal liver. Blood 2007;110:2889–2898. [PubMed: 17644732]

Chou YT, Wang H, Chen Y, Danielpour D, Yang YC. Cited2 modulates TGF-beta-mediated upregulation of MMP9. Oncogene 2006;25:5547–5560. [PubMed: 16619037]

Chow RL, Lang RA. Early eye development in vertebrates. Annu Rev Cell Dev Biol 2001;17:255–296. [PubMed: 11687490]

Cramer T, Yamanishi Y, Clausen BE, Forster I, Pawlinski R, Mackman N, Haase VH, Jaenisch R, Corr M, Nizet V, et al. HIF-1alpha is essential for myeloid cell-mediated inflammation. Cell 2003;112:645–657. [PubMed: 12628185]

Davis-Silberman N, Kalich T, Oron-Karni V, Marquardt T, Kroeber M, Tamm ER, Ashery-Padan R. Genetic dissection of Pax6 dosage requirements in the developing mouse eye. Hum Mol Genet 2005;14:2265–2276. [PubMed: 15987699]

Dimanlig PV, Faber SC, Auerbach W, Makarenkova HP, Lang RA. The upstream ectoderm enhancer in Pax6 has an important role in lens induction. Development 2001;128:4415–4424. [PubMed: 11714668]

Donner AL, Episkopou V, Maas RL. Sox2 and Pou2f1 interact to control lens and olfactory placode development. Dev Biol 2007;303:784–799. [PubMed: 17140559]

Dunwoodie SL, Rodriguez TA, Beddington RSP. Msg1 and Mrg1, founding members of a gene family, show distinct patterns of gene expression during mouse embryogenesis. Mech Dev 1998;72:27–40. [PubMed: 9533950]

Flamme I, Breier G, Risau W. Vascular endothelial growth factor (VEGF) and VEGF receptor 2 (flk-1) are expressed during vasculogenesis and vascular differentiation in the quail embryo. Dev Biol 1995;169:699–712. [PubMed: 7781909]

Freedman SJ, Sun ZY, Kung AL, France DS, Wagner G, Eck MJ. Structural basis for negative regulation of hypoxia-inducible factor-1alpha by CITED2. Nat Struct Biol 2003;10:504–512. [PubMed: 12778114]

Glenn DJ, Maurer RA. MRG1 binds to the LIM domain of Lhx2 and may function as a coactivator to stimulate glycoprotein hormone alpha-subunit gene expression. J Biol Chem 1999;274:36159–36167. [PubMed: 10593900]

Goldberg MF. Persistent fetal vasculature (PFV): an integrated interpretation of signs and symptoms associated with persistent hyperplastic primary vitreous (PHPV). LIV Edward Jackson Memorial Lecture. Am J Ophthalmol 1997;124:587–626. [PubMed: 9372715]

Grindley JC, Davidson DR, Hill RE. The role of Pax-6 in eye and nasal development. Development 1995;121:1433–1442. [PubMed: 7789273]

Haddad R, Font RL, Reeser F. Persistent hyperplastic primary vitreous. A clinicopathologic study of 62 cases and review of the literature. Surv Ophthalmol 1978;23:123–134. [PubMed: 100893]

Hanson IM, Fletcher JM, Jordan T, Brown A, Taylor D, Adams RJ, Punnett HH, van Heyningen V. Mutations at the PAX6 locus are found in heterogeneous anterior segment malformations including Peters' anomaly. Nat Genet 1994;6:168–173. [PubMed: 8162071]

Hill RE, Favor J, Hogan BLM, Ton CCT, Saunders GF, Hanson IM, Prosser J, Jordan T, Hastie ND, van Heyningen V. Mouse Small eye results from mutations in a paired-like homeobox-containing gene. Nature 1991;354:522–525. [PubMed: 1684639]

Ito M, Yoshioka M. Regression of the hyaloid vessels and pupillary membrane of the mouse. Anat Embryol 1999;200:403–411. [PubMed: 10460477]

Kammandel B, Chowdhury K, Stoykova A, Aparicio S, Brenner S, Gruss P. Distinct cis-essential modules direct the time-space pattern of the Pax6 gene activity. Dev Biol 1999;205:79–97. [PubMed: 9882499]

Kaufman MH, Chang HH, Shaw JP. Craniofacial abnormalities in homozygous Small eye (Sey/Sey) embryos and newborn mice. J Anat 1995;186:607–617. [PubMed: 7559133]

Kenyon KR. Mesenchymal dysgenesis in Peter's anomaly, sclerocornea and congenital endothelial dystrophy. Exp Eye Res 1975;21:125–142. [PubMed: 1100415]

Kleinjan DA, Seawright A, Schedl A, Quinlan RA, Danes S, van Heyningen V. Aniridia-associated translocations, DNase hypersensitivity, sequence comparison and transgenic analysis redefine the functional domain of PAX6. Hum Mol Genet 2001;10:2049–2059. [PubMed: 11590122]

Kleinjan DA, Seawright A, Elgar G, van Heyningen V. Characterization of a novel gene adjacent to PAX6, revealing synteny conservation with functional significance. Mamm Genome 2002;13:102–107. [PubMed: 11889558]

Kleinjan DA, Seawright A, Mella S, Carr CB, Tyas DA, Simpson TI, Mason JO, Price DJ, van Heyningen V. Long-range downstream enhancers are essential for Pax6 expression. Dev Biol 2006;299:563–581. [PubMed: 17014839]

Leung MK, Jones T, Michels CL, Livingston DM, Bhattacharya S. Molecular cloning and chromosomal localization of the human CITED2 gene encoding p35srj/Mrg1. Genomics 1999;61:307–313. [PubMed: 10552932]

Liu Y, Cox SR, Morita T, Kourembanas S. Hypoxia regulates vascular endothelial growth factor gene expression in endothelial cells: identification of a 5′ enhancer. Circ Res 1995;77:638–643. [PubMed: 7641334]

Mitchell CA, Rutland CS, Walker M, Nasir M, Foss AJ, Stewart C, Gerhardt H, Konerding MA, Risau W, Drexler HC. Unique vascular phenotypes following over-expression of individual VEGFA isoforms from the developing lens. Angiogenesis 2006;9:209–224. [PubMed: 17109192]

Myles WM, Flanders ME, Chitayat D, Brownstein S. Peters' anomaly: a clinicopathologic study. J Pediatr Ophthalmol Strabismus 1992;29:374–381. [PubMed: 1287176]

Pollard ZF. Persistent hyperplastic primary vitreous: diagnosis, treatment and results. Trans Am Ophthalmol Soc 1997;95:487–549. [PubMed: 9440186]

Preis JI, Wise N, Solloway MJ, Harvey RP, Sparrow DB, Dunwoodie SL. Generation of conditional Cited2 null alleles. Genesis 2006;44:579–583. [PubMed: 17133411]

Pugh CW, Ratcliffe PJ. Regulation of angiogenesis by hypoxia: role of the HIF system. Nat Med 2003;9:677–684. [PubMed: 12778166]

Qu X, Lam E, Doughman YQ, Chen Y, Chou YT, Lam M, Turakhia M, Dunwoodie SL, Watanabe M, Xu B, et al. Cited2, a coactivator of HNF4alpha, is essential for liver development. EMBO J 2007;26:4445–4456. [PubMed: 17932483]

Quiring R, Walldorf U, Kloter U, Gehring WJ. Homology of the eyeless gene of Drosophila to the Small eye gene in mice and Aniridia in humans. Science 1994;265:785–789. [PubMed: 7914031]

Rutland CS, Mitchell CA, Nasir M, Konerding MA, Drexler HC. Microphthalmia, persistent hyperplastic hyaloid vasculature and lens anomalies following overexpression of VEGF-A188 from the alphaA-crystallin promoter. Mol Vis 2007;13:47–56. [PubMed: 17277743]

Schedl A, Ross A, Lee M, Engelkamp D, Rashbass P, van Heyningen V, Hastie ND. Influence of PAX6 gene dosage on development: overexpression causes severe eye abnormalities. Cell 1996;86:71–82. [PubMed: 8689689]

Shioda T, Fenner MH, Isselbacher KJ. MSG1 and its related protein MRG1 share a transcription activating domain. Gene 1997;204:235–241. [PubMed: 9434189]

Shui YB, Wang X, Hu JS, Wang SP, Garcia CM, Potts JD, Sharma Y, Beebe DC. Vascular endothelial growth factor expression and signaling in the lens. Invest Ophthalmol Vis Sci 2003;44:3911–3919. [PubMed: 12939309]

Shui YB, Fu JJ, Garcia C, Dattilo LK, Rajagopal R, McMillan S, Mak G, Holekamp NM, Lewis A, Beebe DC. Oxygen Distribution in the Rabbit Eye and Oxygen Consumption by the Lens. Invest Ophthalmol Vis Sci 2006;47:1571–1580. [PubMed: 16565394]

Shweiki D, Itin A, Soffer D, Keshet E. Vascular endothelial growth factor induced by hypoxia may mediate hypoxia-initiated angiogenesis. Nature 1992;359:843–845. [PubMed: 1279431]

Smith GM, Velzeboer CM. Peter's anomaly. Ophthalmologica 1975;171:318–320. [PubMed: 1165907]

Sun HB, Zhu YX, Yin T, Sledge G, Yang YC. MRG1, the product of a melanocyte-specific gene related gene, is a cytokine-inducible transcription factor with transformation activity. Proc Natl Acad Sci USA 1998;95:13555–13560. [PubMed: 9811838]

Tien ES, Davis JW, Vanden Heuvel JP. Identification of the CREB-binding protein/p300-interacting protein CITED2 as a peroxisome proliferator-activated receptor alpha coregulator. J Biol Chem 2004;279:24053–24063. [PubMed: 15051727]

Val P, Martinez-Barbera JP, Swain A. Adrenal development is initiated by Cited2 and Wt1 through modulation of Sf-1 dosage. Development 2007;134:2349–2358. [PubMed: 17537799]

van Raamsdonk CD, Tilghman SM. Dosage requirement and allelic expression of PAX6 during lens placode formation. Development 2000;127:5439–5448. [PubMed: 11076764]

Walther C, Gruss P. Pax-6, a murine paired box gene, is expressed in the developing CNS. Development 1991;113:1435–1449. [PubMed: 1687460]

Weninger WJ, Floro KL, Bennett MB, Withington SL, Preis JI, Barbera JP, Mohun TJ, Dunwoodie SL. Cited2 is required both for heart morphogenesis and establishment of the left-right axis in mouse development. Development 2005;132:1337–1348. [PubMed: 15750185]

West-Mays JA, Zhang J, Nottoli T, Hagopian-Donaldson S, Libby D, Strissel KJ, Williams T. AP-2alpha transcription factor is required for early morphogenesis of the lens vesicle. Dev Biol 1999;206:46–62. [PubMed: 9918694]

Williams SC, Altmann CR, Chow RL, Hemmati-Brivanlou A, Lang RA. A highly conserved lens transcriptional control element from the Pax-6 gene. Mech Dev 1998;73:225–229. [PubMed: 9622640]

Withington SL, Scott AN, Saunders DN, Lopes FK, Preis JI, Michalicek J, Maclean K, Sparrow DB, Barbera JP, Dunwoodie SL. Loss of Cited2 affects trophoblast formation and vascularization of the mouse placenta. Dev Biol 2006;294:67–82. [PubMed: 16579983]

Xu B, Doughman Y, Turakhia M, Jiang W, Landsettle CE, Agani FH, Semenza GL, Watanabe M, Yang YC. Partial rescue of defects in Cited2-deficient embryos by HIF-1alpha heterozygosity. Dev Biol 2007;301:130–140. [PubMed: 17022961]

Xu PX, Zhang X, Heaney S, Yoon A, Michelson AM, Maas RL. Regulation of Pax6 expression is conserved between mice and flies. Development 1999;126:383–395. [PubMed: 9847251]

Yang Y, Cvekl A. Tissue-specific regulation of the mouse alphaA-crystallin gene in lens via recruitment of Pax6 and c-Maf to its promoter. J Mol Biol 2005;19:453–469. [PubMed: 16023139]

Yang Y, Stopka T, Golestaneh N, Wang Y, Wu K, Li A, Chauhan BK, Gao CY, Cveklova K, Duncan MK, et al. Regulation of alphaA-crystallin via Pax6, c-Maf, CREB and a broad domain of lens-specific chromatin. EMBO J 2006;25:2107–2118. [PubMed: 16675956]

Yin Z, Haynie J, Yang X, Han B, Kiatchoosakun S, Restivo J, Yuan S, Prabhakar NR, Herrup K, Conlon RA, et al. The essential role of Cited2, a negative regulator for HIF-1alpha, in heart development and neurulation. Proc Natl Acad Sci USA 2002;99:10488–10493. [PubMed: 12149478]

Yoon G. Neonatal corneal opacity: a case study of Peters' anomaly. Neonatal Netw 2001;20:65–72. [PubMed: 12144118]

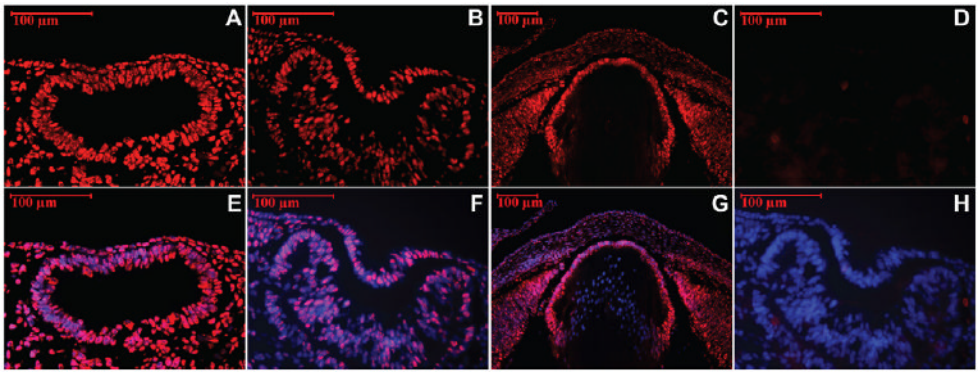

Fig. 1. Cited2 is expressed in the developing mouse lens

Immunostaining for Cited2 on eye sections from various developmental stages. Cited2 expression (red) was detected in the surface ectoderm at 9.5 dpc (**A**), invaginating lens placode at 10.5 dpc (**B**), and in lens epithelial cells at 15.5 dpc (**C**), but not in the negative control (**D**). Cited2 immunostaining (red) (**E-G**) and negative control (**H**) from corresponding stages were merged with DAPI nuclei staining (blue).

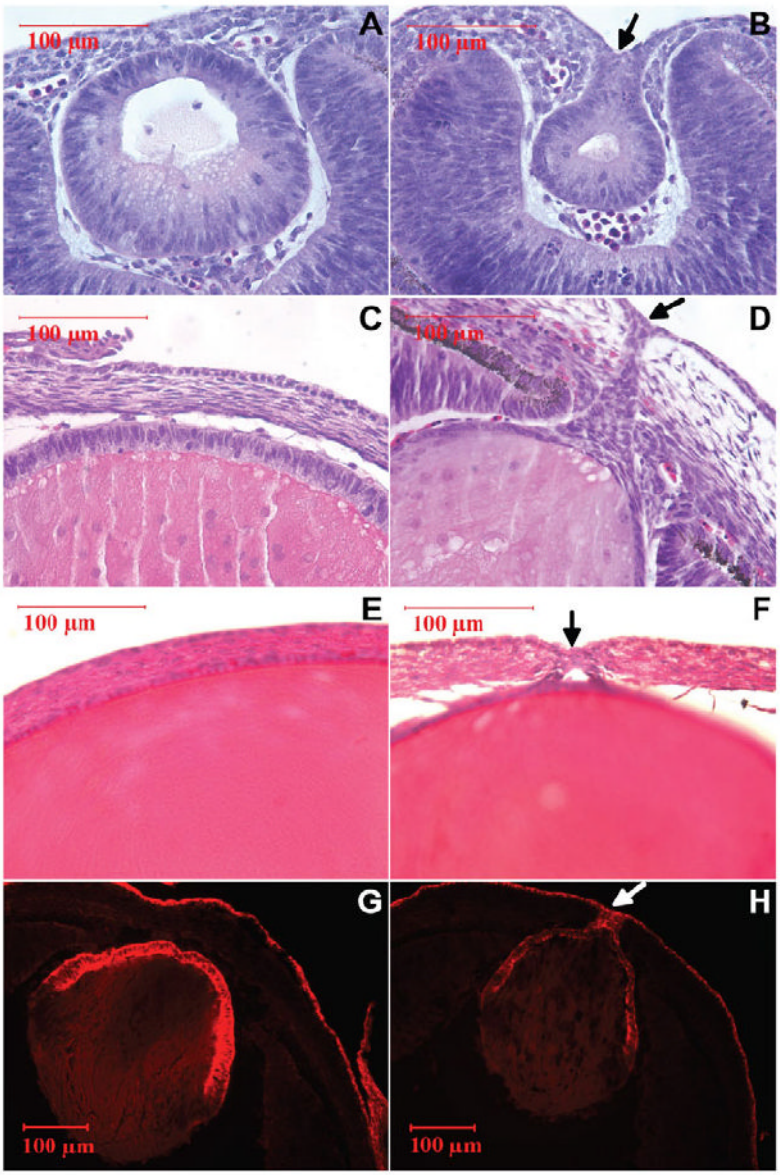

Fig. 2. Formation of the lens stalk in *Cited2*$^{-/-}$ eyes

(**A-F**) Histological examination was performed after Hematoxylin and Eosin (H&E) staining of serial paraffin sections of mouse embryo heads. Compared with wild-type littermate controls at corresponding stages (A,C,E), fusion of the lens to the surface ectoderm was detected at 11.5 dpc (arrow in B) and the resultant lens stalk persisted throughout development as shown in representative pictures from 15.5 (arrow in D) and 18.5 dpc (arrow in F) in *Cited2*$^{-/-}$ eyes. (**G**,**H**) E-cadherin immunostaining was performed on sections from 13.5 dpc. In contrast to the expression in corneal epithelium and lens epithelial cells in the wild-type littermate control (G), positive E-cadherin staining for lens stalk was revealed in *Cited2*$^{-/-}$ eyes (arrow in H).

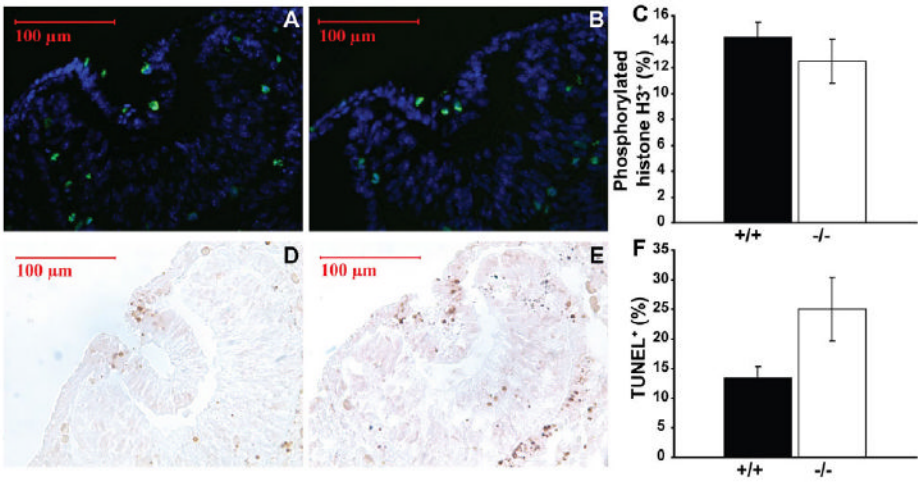

Fig. 3. Proliferation and cell death in *Cited2*$^{-/-}$ lens

(**A-C**) Proliferation of the developing mouse lens at 10.5 dpc was examined by phosphorylated histone H3 immunostaining (green) and counterstained with DAPI (blue). No significant difference in proliferation was detected between *Cited2*$^{+/+}$ littermate controls (A) (*n*=3) and *Cited2*$^{-/-}$ lens (B) (*n*=5); the data are summarized in C (*P*>0.05). (**D-F**) Cell death of the developing lens at 10.5 dpc was examined by the TUNEL assay. For counting cell number, sections were counterstained with DAPI to reveal nuclei (data not shown). Compared with *Cited2*$^{+/+}$ littermate controls (D) (*n*=3), increased cell death was observed in *Cited2*$^{-/-}$ lens (E) (*n*=5); the data are summarized in F (*P*<0.01).

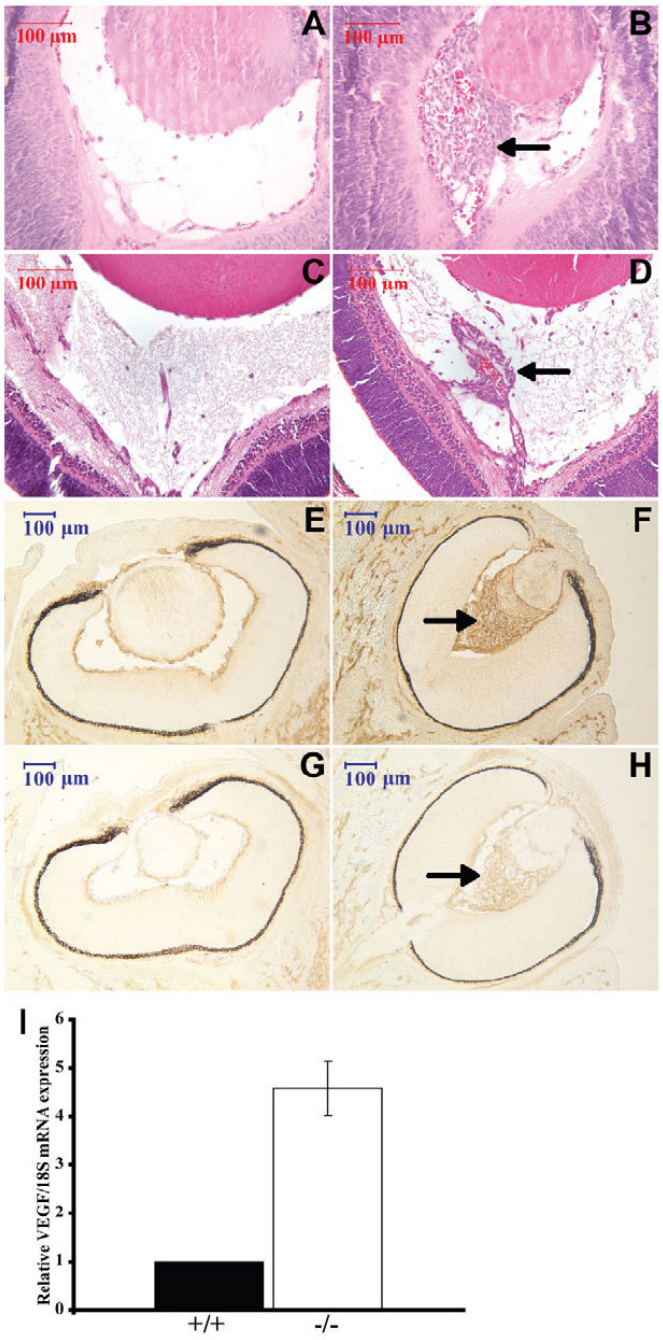

Fig. 4. Hyaloid hypercellularity and aberrant vasculature in *Cited2*$^{-/-}$ eyes

(**A-D**) Histological examination was performed after H&E staining of serial paraffin sections of mouse embryo heads. The analysis revealed hyaloid hypercellularity and aberrant vasculature in *Cited2*$^{-/-}$ eyes at 15.5 (arrow in B) and 18.5 (arrow in D) dpc, in comparison to normal intraocular vasculature in wild-type littermate controls at 15.5 (A) and 18.5 (C) dpc. (**E-H**) The abnormal vasculature was further confirmed by immunostaining *Cited2*$^{-/-}$ eye sections at 15.5 dpc for endothelial cells by CD31 (arrow in F) and endothelial and angioblast cells by VEGFR2 (arrow in H), as compared with normal expression patterns for CD31 (E) and VEGFR2 (G) in wild-type controls. (**I**) *Vegf* mRNA expression was increased in

Cited2$^{-/-}$ lens (*n*=4) compared with the wild-type littermate control (*n*=4), as quantified by real-time PCR analysis.

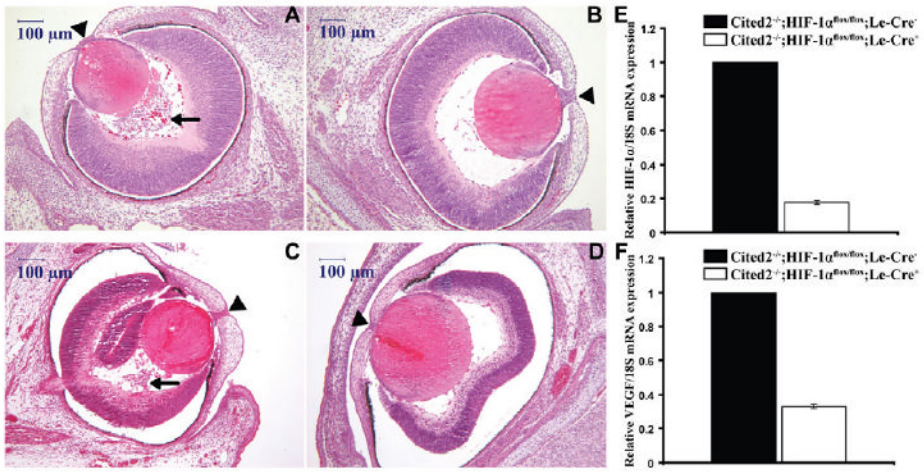

Fig. 5. Deletion of *Hif1a* in the lens specifically eliminates the hyaloid hypercellularity and aberrant vasculature of *Cited2*$^{-/-}$ eyes

(**A-D**) H&E-stained serial paraffin sections of mouse embryo heads at 15.5 and 17.5 dpc revealed that at both stages, *Cited2*$^{-/-}$;*Hif1a*$^{flox/flox}$;*Le-Cre*$^{-}$ eyes displayed lens stalk formation (arrowhead in A,C) and hyaloid hypercellularity with aberrant vasculature (arrow in A,C) (*n*=3). In *Cited2*$^{-/-}$;*Hif1a*$^{flox/flox}$;*Le-Cre*$^{+}$ eyes (*n*=3), only the lens stalk (arrowhead in B,D), but not the hyaloid hypercellularity, was detected. Data shown are representative of three independent litters examined. (**E**) *Le-Cre* transgene-mediated deletion of *Hif1a* was assessed by real-time PCR analysis of *Hif1a* mRNA expression at 14.5 dpc, which revealed a 5-fold decrease in the *Hif1a* mRNA level in *Cited2*$^{-/-}$;*Hif1a*$^{flox/flox}$;*Le-Cre*$^{+}$ lens (*n*=3) compared with the level detected in *Cited2*$^{-/-}$;*Hif1a*$^{flox/flox}$;*Le-Cre*$^{-}$ lens (*n*=3). (**F**) As a consequence, *Vegf* mRNA expression decreased about 3-fold in *Cited2*$^{-/-}$;*Hif1a*$^{flox/flox}$;*Le-Cre*$^{+}$ lens (*n*=3) compared with the level detected in *Cited2*$^{-/-}$;*Hif1a*$^{flox/flox}$;*Le-Cre*$^{-}$ lens (*n*=3).

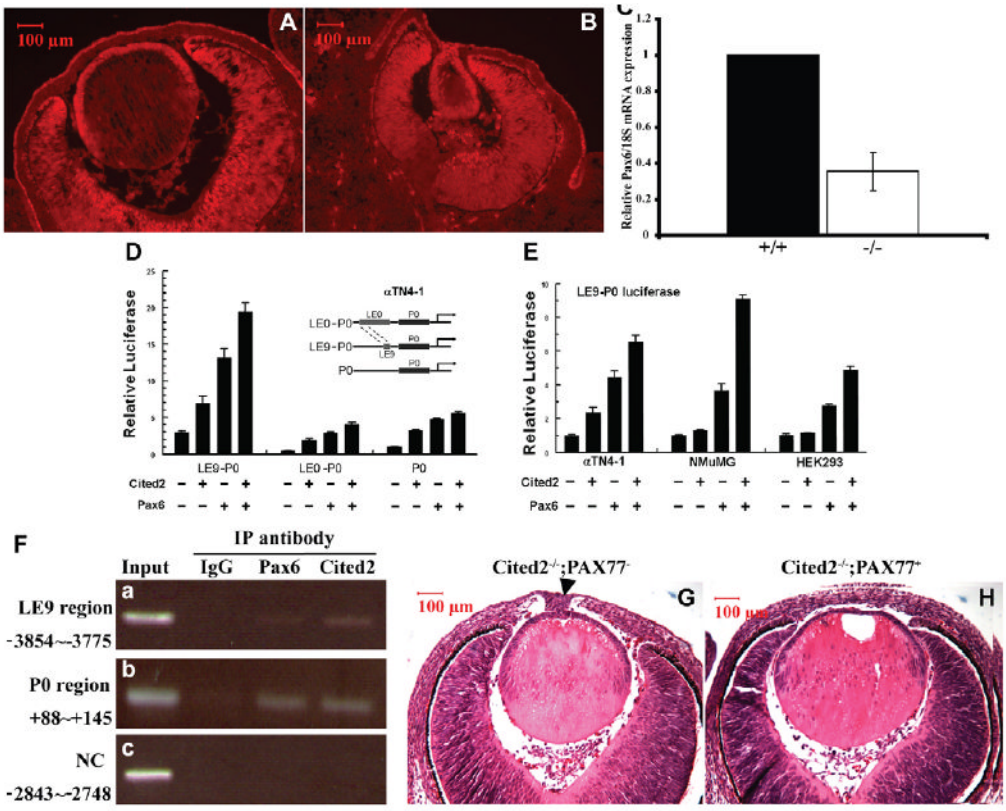

Fig. 6. Cited2 is a positive regulator for Pax6 expression

(**A**,**B**) Expression of Pax6 in *Cited2*$^{-/-}$ lens epithelial cells. Immunostaining revealed an appreciable level of Pax6 expression in *Cited2*$^{-/-}$ lens epithelial cells at 13.5 dpc (B) compared with that of wild-type littermate controls (A). (**C**) *Pax6* mRNA expression in developing lens at 14.5 dpc was analyzed by real-time PCR, which revealed a 2.5-fold reduction of *Pax6* expression in *Cited2*$^{-/-}$ lens (n=4) as compared with wild-type littermate controls (n=4). (**D**,**E**) Effect of Cited2 on Pax6 autoregulation. Transcriptional activation of reporters containing *Pax6* enhancer and promoter fragments, LE9-P0, LE0-P0 and P0, in Cited2- or Pax6-overexpressing cells was measured by reporter assays. α-TN4-1 mouse lens epithelial cells were transfected with a reporter plasmid containing the indicated fragment (270 ng) with different combinations of Cited2 (225 ng) and Pax6 (75 ng) expression plasmids. Cited2 overexpression in Pax6-expressing α-TN4-1 cells significantly increased the activity of LE9-P0, LE0-P0 and P0 reporters (D). This effect was Pax6-dependent because Cited2 overexpression had no effect on LE9-P0 reporter activity in NMuMG and HEK293 cells, which do not express Pax6, but co-expression of Pax6 and Cited2 significantly increased the reporter activity (E). (**F**) Cited2 is present on the *Pax6* promoter. ChIP assays were performed using 2×10^6 α-TN4-1 cells and antibodies against Cited2 and Pax6. The precipitated DNA was analyzed by PCR with primers covering the LE9 ectoderm enhancer and the P0 promoter region. Normal mouse IgG and PCR amplifying the sequence between LE9 and P0 were also included as negative controls. Input was 10% of the chromatin for immunoprecipitation. Representative pictures show occupancy of Cited2 on LE9 (**a**) and P0 region (**b**) as compared with the negative control (NC) (**c**). (**G**,**H**) Histological examination was performed after H&E staining of paraffin-embedded eye serial sections collected from *Cited2*$^{-/-}$;PAX77^{-} and *Cited2*$^{-/-}$;PAX77^{+} littermates at 14.5 dpc. Abnormal lens stalk formation was consistently detected in *Cited2*$^{-/-}$;PAX77^{-} embryonic eyes (n=2) (arrowhead in G). However, no lens stalk

was detected in any of the serial sections collected from *Cited2*$^{-/-}$;PAX77^{+} mouse embryos (*n*=3) (H).

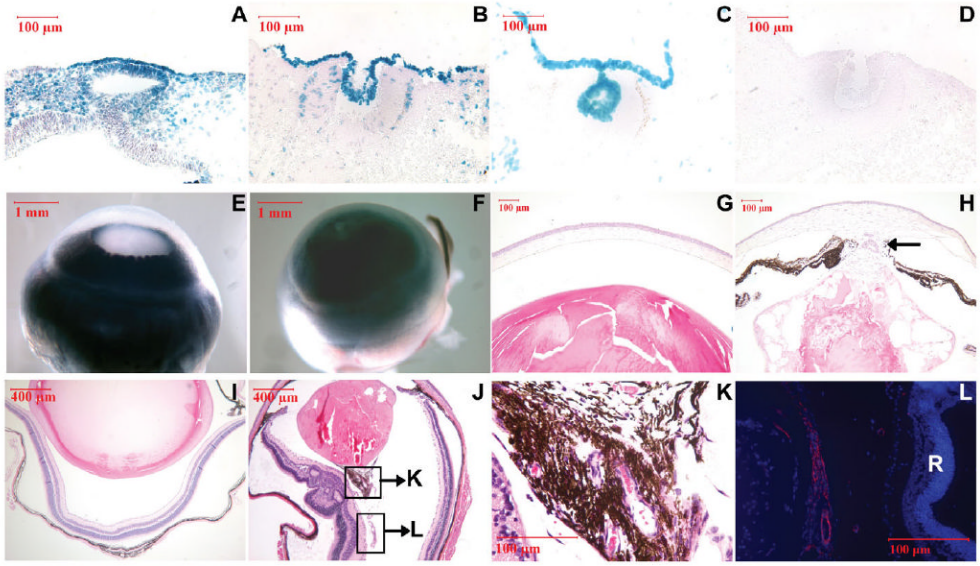

Fig. 7. Le-Cre-mediated deletion of *Cited2*

(**A-D**) *Le-Cre* transgene-mediated recombination of floxed *Cited2* alleles was revealed by *lacZ* staining in *Cited2*$^{flox/flox}$;*Le-Cre*$^{+}$ developing mouse lens at 9.5 (A), 10.5 (B) and 11.5 (C) dpc, which is in contrast to the negative *lacZ* staining pattern in *Cited2*$^{flox/flox}$;*Le-Cre*$^{-}$ control eyes (D). (**E**,**F**) Macroscopic examination revealed smaller eyes and failure to form the anterior chamber in *Cited2*$^{flox/flox}$;*Le-Cre*$^{+}$ embryos (F) as compared with those from *Cited2*$^{flox/flox}$;*Le-Cre*$^{-}$ embryos (E) at 6 weeks of age. (**G-L**) H&E staining of cross-sections revealed failed separation of the lens from the cornea in *Cited2*$^{flox/flox}$;*Le-Cre*$^{+}$ eyes (arrow in H) as compared with the normal histology in *Cited2*$^{flox/flox}$;*Le-Cre*$^{-}$ eyes (G) at 6 weeks of age. In addition, abnormal retrolenticular tissue (boxed) was also detected in *Cited2*$^{flox/flox}$;*Le-Cre*$^{+}$ eyes (J) as compared with *Cited2*$^{flox/flox}$;*Le-Cre*$^{-}$ controls (I). Higher magnification of boxed retrolenticular tissue from J shows melanocytes and aberrant blood vessels (K). Immunostaining for α-SMA (red) and counterstaining with DAPI (blue) demonstrates α-SMA-positive pericytes surrounding the blood vessels in *Cited2*$^{flox/flox}$;*Le-Cre*$^{+}$ eyes (L). R, retina.

Table 1

Summary of ocular phenotypes in Cited2-deficient embryos

Stage dpc*	Irregular pupil†	Small lens pit/lens†	Lens stalk†	Aberrant vasculature†
10.5 (4)	N/A	4	N/A	N/A
11.5 (4)	N/A	4	4	4
12.5 (10)	N/A	10	10	10
13.5 (16)	16	16	16	16
14.5 (10)	10	10	10	10
15.5 (10)	10	10	10	10
18.5 (12)	12	12	12	12

*The number of embryos analyzed is indicated in parentheses.

†The number of embryos identified with the indicated defect.

N/A, not applicable.